Radiative $ggg \leftrightarrow gg$ transport and thermalization †

Dustin Hemphill and Denes Molnar

Department of Physics and Astronomy, Purdue University, West Lafayette, IN 47907, U.S.A.

Abstract: The mechanism of rapid thermalization in heavy-ion reaction is still an open problem. While $2 \to 2$ perturbative QCD rates do not thermalize sufficiently fast (e.g., [1]), it has been claimed a decade ago[2] based on the BAMPS code that perturbative $ggg \leftrightarrow gg$ rates shorten thermalization time-scales in $A + A$ at RHIC and LHC energies to ~ 1 fm/c or smaller. Later it has been argued, however, (e.g., [3]) that the BAMPS calculation may have missed the rates by a factor of $3! = 6$. We investigate the thermalization question using the transport code MPC/Grid, which algorithmically is quite similar to BAMPS (it has scatterings implemented via sampling test particles in small spatial cells in discrete timesteps). The new code has been verified against every analytic test we could think of, and in $2 \to 2$ mode also against earlier $A + A$ results from the geometric MPC/Cascade code. On one hand, we do find that the inclusion of $ggg \leftrightarrow gg$ rates speeds up thermalization very significantly, however, the rates are still not as high as those published from BAMPS. The difference in $3 \leftrightarrow 2$ rates, however, is not simply a factor of 6 even when we try to reproduce their calculation. On the other hand, we do find that the $ggg \leftrightarrow gg$ rates are very sensitive to how screening and the LPM effect are implemented. Results from MPC/Grid for collective flow in $A + A$ reactions are also discussed.

Covariant transport with $2 \to 2$ and $3 \leftrightarrow 2$

For massless *on-shell* gluons with $2 \to 2$ and $3 \leftrightarrow 2$ interactions, the Boltzmann limit of covariant transport is

$$p_1^\mu \partial_\mu f(x,\vec{p}_1) = \frac{1}{128\pi^2} \iiint\limits_{2\,3\,4} (f_3 f_4 - f_1 f_2)\, |\bar{\mathcal{M}}_{12\to34}|^2 \delta^4(12-34)$$
$$+ \frac{1}{3!\,1024\pi^5} \iiiint\limits_{2\,3\,4\,5} \left(\frac{(2\pi)^3}{\hat g} f_3 f_4 f_5 - f_1 f_2 \right) |\bar{\mathcal{M}}_{12\to345}|^2 \delta^4(12{-}345)$$
$$+ \frac{1}{2!\,2048\pi^5} \iiiint\limits_{2\,3\,4\,5} \left(f_4 f_5 - \frac{(2\pi)^3}{\hat g} f_1 f_2 f_3 \right) |\bar{\mathcal{M}}_{45\to123}|^2 \delta^4(123{-}45)\,.$$

Here $f_i \equiv f(x,\vec{p}_i)$, $\int_i \equiv \int d^3p_i/E_i$, $\delta^4(i...j-k...l) \equiv \delta^4(p_i + ... + p_j - p_k - ... - p_l)$, $|\bar{\mathcal{M}}|^2$ denotes the respective *unpolarized* $2 \to 2$, $2 \to 3$ and $3 \to 2$ scattering matrix elements, and $\hat g = 16$ is the number of internal degrees for freedom for gluons. This equation can equilibrate both thermally and chemically (in static box).

Total $2 \to 3$ cross section and thermal rates

We use matrix elements based on leading-order (LO) perturbative QCD. For $2 \to 2$:

$$|\bar{\mathcal{M}}_{gg\to gg}|^2 = \frac{9g^4}{2}\left(3 - \frac{ut}{s^2} - \frac{us}{t^2} - \frac{ts}{u^2}\right) \approx \frac{9g^4 s^2}{2}\left(\frac{1}{t^2} + \frac{1}{u^2}\right)$$

in the small angle scattering limit. For $2 \leftrightarrow 3$ [4]:

$$|\bar{\mathcal{M}}_{gg\to ggg}|^2 = \frac{g^6 N_c^3}{2(N_c^2-1)} \sum_{perms\{12345\}} \frac{1}{p_{12}\,p_{23}\,p_{34}\,p_{45}\,p_{51}} \times \sum_{i<j} p_{ij}^4\,, \qquad p_{ij} \equiv p_i p_j\,.$$

Divergences for collinear momenta are alleviated by screening in the medium. For $2 \to 2$ we implement simple Debye screening via $1/t^2 \to 1/(t - \mu_D^2)^2$. For $2 \leftrightarrow 3$, we analogously shift $p_i p_j \to p_i p_j + \mu_D^2$ in denominators (similar to Ref. [3]). From linear response theory[5], $\mu_D^2[f] = 3\pi\alpha_s \int d^3p \frac{1}{p} f(\vec{p})$. Note that with Bose statistics this gives $\mu_D = gT$, while with classical statistics the 30% smaller value $\mu_D = \sqrt{6/\pi^2}\, gT$.

For comparisons with BAMPS, we also consider the $2 \to 3$ matrix element in the Bertsch-Gunion (BG) limit: $|\bar{\mathcal{M}}_{gg\to ggg}|^2_{BG} = 54 g^6 s^2 / \vec{q}_T^{\,2} \vec{k}_T^{\,2} (\vec{k}_T + \vec{q}_T)^2$ (with $N_c = 3$), where $\vec{k}_T$ and $\vec{q}_T$ are 2D transverse momenta of two of the outgoing gluons in the CM frame of the $2 \to 3$ scattering, relative to the axis of incoming momenta. We explore different ways to regulate the denominator:

$$\text{symmetric BG}: \quad \frac{1}{(\vec{q}_T^{\,2} + \mu_D^2)\,(\vec{k}_T^{\,2} + \mu_D^2)\,[(\vec{k}_T + \vec{q}_T)^2 + \mu_D^2]}$$
$$\text{BG}: \quad \frac{\vec{q}_T^{\,2}}{(\vec{q}_T^{\,2} + \mu_D^2)^2\,(\vec{k}_T^{\,2} + \mu_D^2)\,[(\vec{k}_T + \vec{q}_T)^2 + \mu_D^2]}$$
$$\text{BG with LPM (BAMPS)}: \quad \frac{\vec{q}_T^{\,2}\,\Theta(k_T - \Lambda)}{(\vec{q}_T^{\,2} + \mu_D^2)^2\,\vec{k}_T^{\,2}\,[(\vec{k}_T + \vec{q}_T)^2 + \mu_D^2]}\,,$$

where Λ is the rate of scattering for a gluon in the medium. Note that the last two forms do not preserve the permutation symmetry over outgoing gluons.

Fig. 1 shows the **total $2 \to 3$ cross section**

$$\sigma_{23}^{TOT} = \frac{1}{3!}\frac{1}{512\pi^5 s} \iiint\limits_{3\,4\,5} |\bar{\mathcal{M}}_{12\to345}|^2 \delta^4(12{-}345)$$

in the various cases, with a natural factor α_s^3/μ_D^2 conveniently removed in the plots. First, we see that the cross section varies sharply with μ_D for $\mu_D/s \lesssim 0.1$. For "symmetric BG" we also calculated for low μ_D/s analytically: $\sigma_{symBG}^{TOT} = \alpha_s^3/\mu_D^2 \times [31.64 \ln(1/z) - 35.80 + ...]$. Second, except for $\mu_D^2/s \sim 0.1$, Bertsch-Gunion is not very accurate. This is even true for the "improved" matrix element $BG \to BG \times [1 - k_T e^{-|y|}/\sqrt{s}]^2$ of Ref. [6] (magenta). Third, the right panel shows that σ_{23}^{TOT} changes significantly if we implement screening via sharp cutoffs $\Theta(p_i p_j - \mu_D^2)$ instead of shifting the poles.

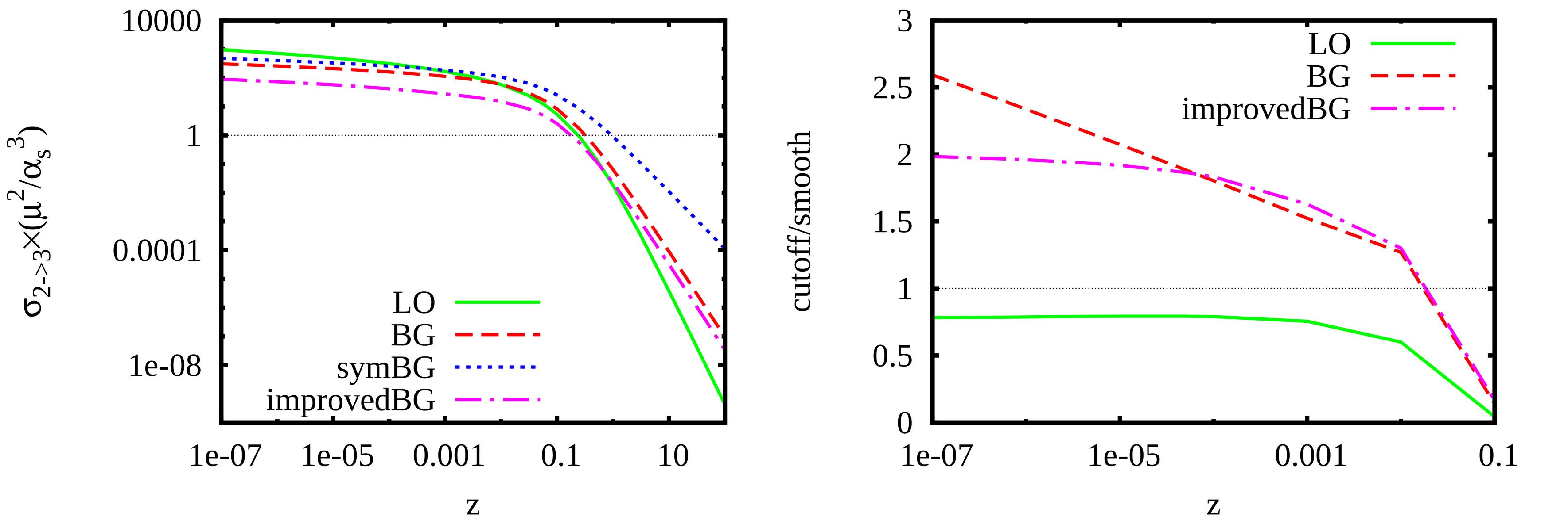

FIGURE 1: Total $2 \to 3$ cross section vs $z = \mu_D^2/s$. *Left:* comparison between full LO and the Bertsch-Gunion limit. *Right:* ratio of $2 \to 3$ cross sections with sharp cutoffs and smooth shift regulators.

Fig. 2 shows $2 \to X$ **gluon scattering rates** $R_{2\to X} \equiv (2/n) \int d^3p_1 d^3p_2 f_1 f_2 v_{rel} \sigma_{2\to X}$ for a **static box in thermal and chemical equilibrium**, with $\alpha_s = 0.3$ and $\mu_D = gT$. We find large variations in the $2 \to 3$ rate depending on the matrix element and screening method used. Nevertheless, unlike Ref. [2] (right panel), in all cases we studied the $2 \to 3$ rate is significantly below the $2 \to 2$ rate. This is so even for "BG with LPM" (solid black line), which we understand to be the practically the same scenario as Ref. [2]. The difference is *not* in μ_D because Ref. [2] used $\mu_D = \sqrt{10/\pi^2}\, gT \approx gT$ too (classical statistics with two quark flavors in their case). If we include $3 \to 2$ rates in the Landau-Pomeranchuk-Migdal suppression factor $\Theta(k_T - \Lambda)$, i.e., take $\Lambda = R_{22} + 2.5 R_{23}$, the rate gets even smaller by about 20% (not shown).

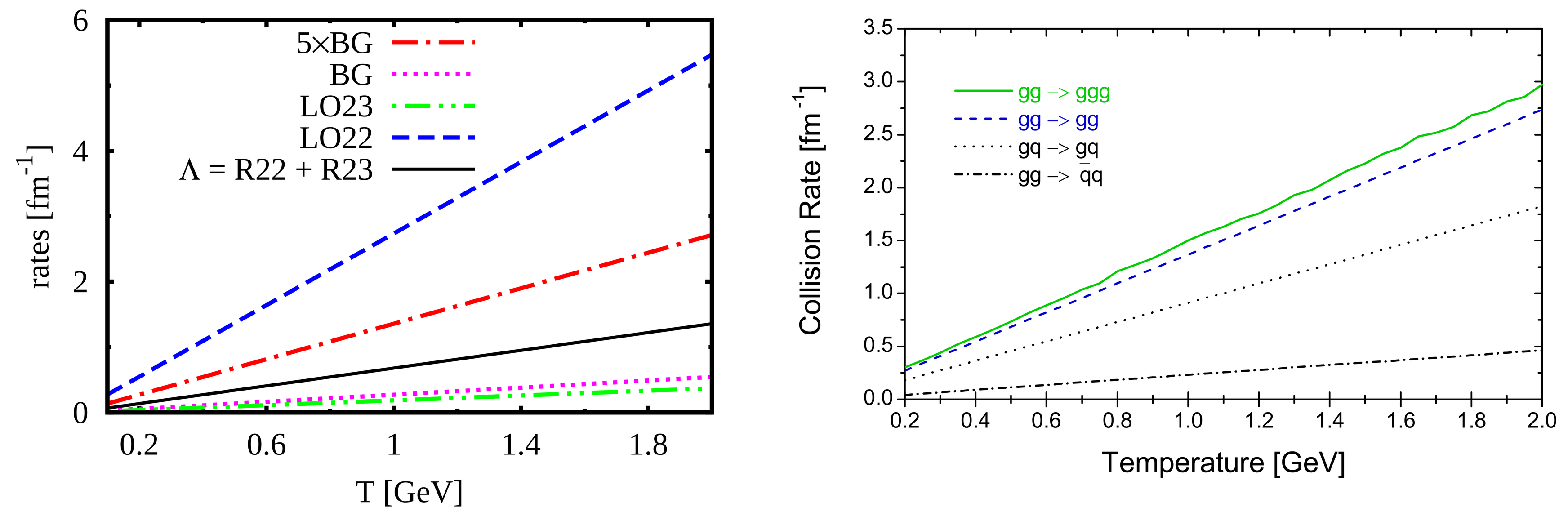

FIGURE 2: Thermal two-body rates from MPC/Grid (left) and BAMPS (right).

Equilibration rate and elliptic flow

Fig. 3 shows **equilibration of the energy (momentum magnitude) distribution** for $\alpha_s = 0.4$ in a static box with initially highly nonthermal, purely transverse spectrum of LO pQCD jets at $\sqrt{s_{NN}} = 200$ GeV with cutoff $p_T > 1.2$ GeV. The density is 25/fm^3, corresponding roughly to the middle of a central Au+Au collision at $\tau = 0.6$ fm for gluon rapidity density $dN_g/d\eta = 1100$ (also close to chemical equilibrium). The left panel shows evolution with $2 \to 2$ scattering only. The right panel includes radiative $gg \leftrightarrow ggg$ (symmetric BG) as well, which speeds equilibration up by about a factor of two (the distribution at time $t/2$ looks close to that at t with $2 \to 2$ only). Both cases use dynamical Debye masses determined from the actual phase space distributions, which accelerates equilibration significantly in *both* cases compared to using the asymptotic ($t \to \infty$) Debye mass.

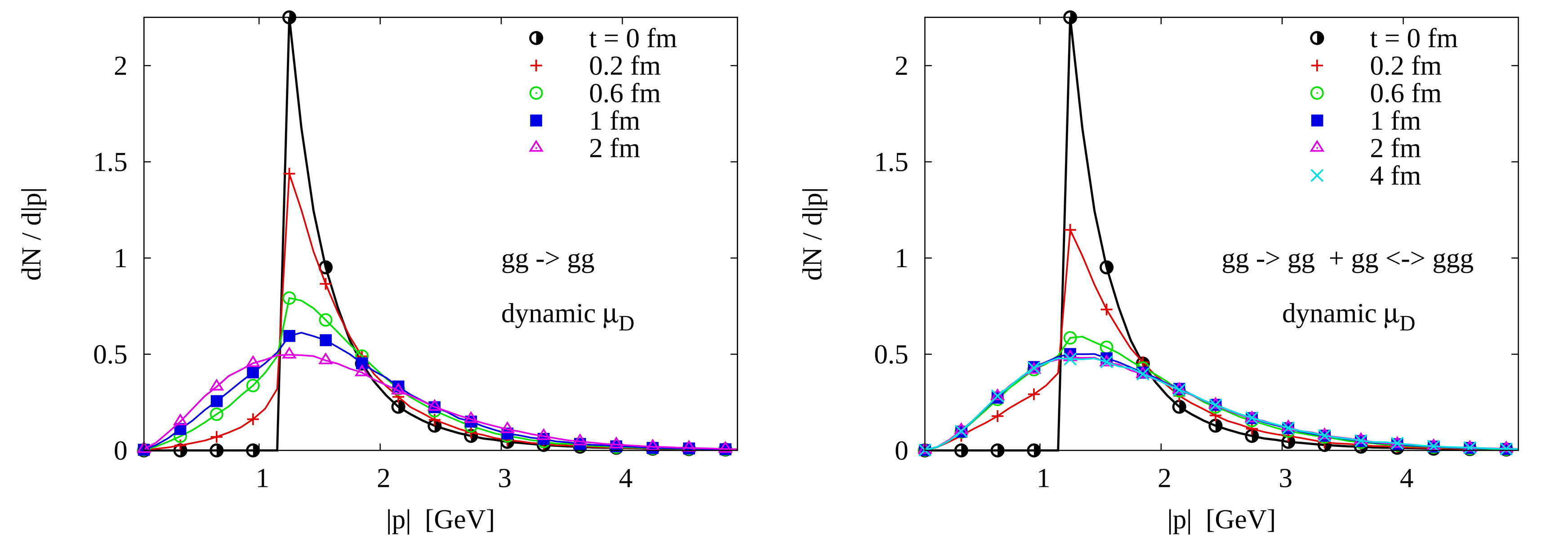

FIGURE 3: Equilibration of the energy distribution as a function of time in a static box with $gg \to gg$ only (left) and both $gg \to gg$ and $gg \leftrightarrow ggg$ (right).

Finally, Fig. 4 shows the **final gluon elliptic flow $v_2(p_T)$ in $Au + Au$ at $b = 8$ fm** for boost-invariant evolution with $\alpha_s = 0.4$ from locally thermal initial conditions with binary collision transverse profile (same initial conditions as in Ref. [7]). Note that the v_2 calculation used the correct energy ($\sqrt{s}$) dependence in rates but generated isotropic outgoing phasespace (for speed), which likely overestimates collective effects. The left panel shows that $gg \leftrightarrow ggg$ can generate large $v_2 \sim 0.1$, mainly due to the dynamical Debye mass in the calculation. The right panel shows that $2 \to 2$ evolution with constant $\sigma_{gg} = 10$ and 20 mb reproduces earlier results from the MPC/Cascade algorithm (scatterings at closest approach).

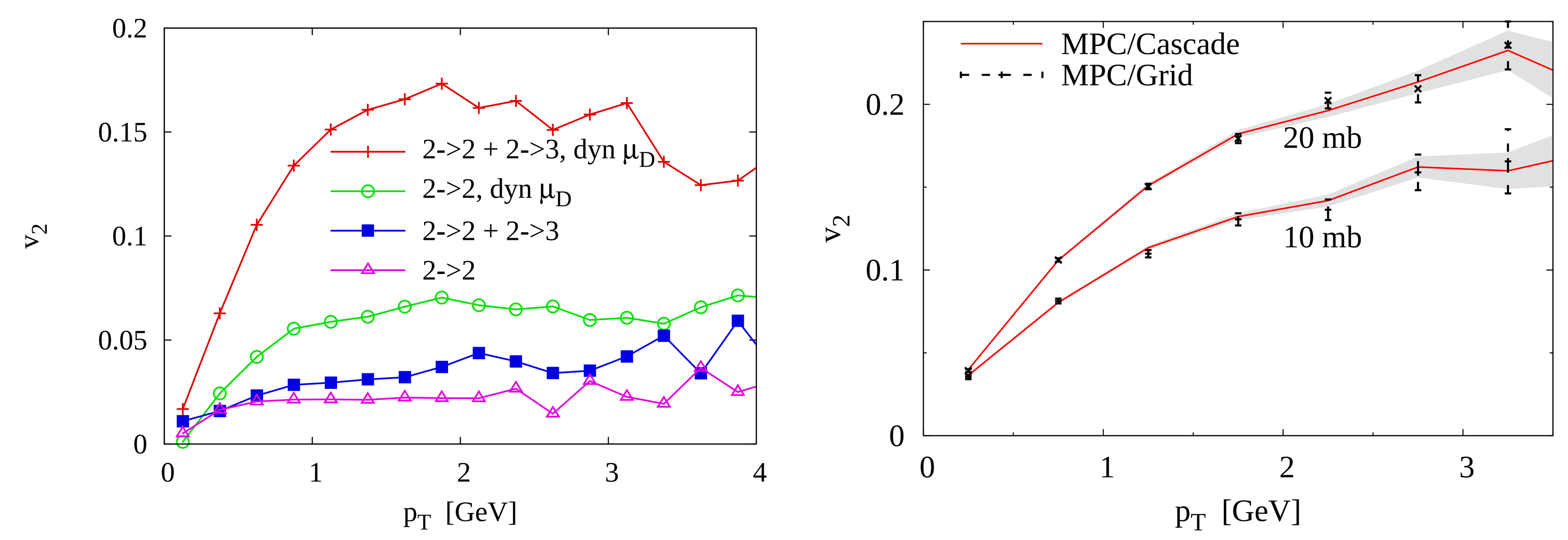

FIGURE 4: Final ($t \to \infty$) gluon $v_2(p_T)$ in $Au + Au$ at $\sqrt{s_{NN}}$ at RHIC, $b = 8$ fm with pQCD cross sections (left) and energy independent cross sections (right).

References:

[1] D. Molnar and M. Gyulassy, Nucl. Phys. A **697**, 495 (2002) [Nucl. Phys. A **703**, 893 (2002)] [nucl-th/0104073].

[2] Z. Xu and C. Greiner, Phys. Rev. C **71**, 064901 (2005) [hep-ph/0406278].

[3] J. W. Chen *et al*, Phys. Lett. B **685**, 277 (2010) [arXiv:0907.2486 [nucl-th]]; Phys. Rev. D **83**, 034031 (2011) [Phys. Rev. D **84**, 039902 (2011)] [arXiv:1011.4123 [hep-ph]].

[4] F. A. Berends *et al* Phys. Lett. B **103**, 124 (1981).

[5] T. S. Biro *et al*, Phys. Rev. C **48**, 1275 (1993) [nucl-th/9303004].

[6] O. Fochler *et al* Phys. Rev. D **88**, no. 1, 014018 (2013) [arXiv:1302.5250 [hep-ph]].

[7] D. Molnar and P. Huovinen, Phys. Rev. Lett. **94**, 012302 (2005) [nucl-th/0404065].

† This work was supported by the US DOE under grant DE-PS02-09ER41665.